Available online at www.sciencedirect.com
SCIENCE DIRECT®
ELSEVIER
Journal of Nuclear Materials 323 (2003) 341–345
journal of nuclear materials
www.elsevier.com/locate/jnucmat

Gas bubbles evolution peculiarities in ferritic–martensitic and austenitic steels and alloys under helium-ion irradiation

I.I. Chernov *, A.N. Kalashnikov, B.A. Kalin, S.Yu. Binyukova

Moscow Engineering Physics Institute (State University), 31 Kashirskoye sh., Moscow 115409, Russian Federation

Abstract

Transmission electron microscopy has been used to investigate the gas bubble evolution in model alloys of the Fe–C system, ferritic–martensitic steels of 13Cr type, nickel and austenitic steels under 40-keV helium-ion irradiation up to a fluence of 5×10^{20} m^{-2} at the temperature of 920 K. It was shown that helium-ion irradiation at high temperature resulted in formation of bubbles with a greater size and a smaller density in Fe and ferritic–martensitic steels than those in nickel and austenitic steels. Large gaseous bubbles in ferritic component are uniformly distributed in grains body in Fe–C alloys as well as in ferritic–martensitic steels. The bubbles with a higher density and a smaller size than those in ferritic component are formed in martensitic grains of steels and Fe–C alloys with a high carbon content ($N_C > 0.01$ wt%), which leads to a small level of swelling of martensite in comparison with that of ferrite. In addition, the bubbles in martensitic grains have a tendency to ordered distribution.

PACS: 61.80

1. Introduction

Austenitic and ferritic–martensitic steels of the Cr13 type are considered as candidate structural materials for the fusion reactors first wall. A significant quantity of helium will be accumulated in the structural materials via (n,α) or other transmutation reactions, it may be implanted from plasma as well as by the absorption of tritium which is β-radioactive isotope and with a decay period of 12.26 years, which results to the formation of a helium isotope ^{3}He. Helium can have a pronounced effect on the radiation damage of materials and often may be an important reason in catastrophic degradation of their properties and shortening of the useful life of reactor constructional elements. In this connection considerable attention has been given to the helium problem in fission and fusion materials. One of these problems is the role of helium in enhancement of radiation swelling.

The goal of this paper is to investigate the peculiarities of gas swelling at high helium concentration and to compare the gaseous swelling level for materials with bcc and fcc structures.

2. Experimental procedure

Nickel and Fe–C model alloys (with carbon concentration $N_C = 0.002\ldots0.4$ wt%) were prepared from high-purity components according to the technique described earlier [1]. After repeated rolling with intermediate homogenizing annealing the samples of model alloys were quenched into iced water from 1370 K after their exposure for 1 h. The compositions of commercial austenitic and ferritic–martensitic steels are presented in Table 1. These steels were applied in two initial conditions: quenching from 1320 K after exposure for 1 h; quenching followed by annealing at 990 K for 0.5 h.

* Corresponding author. Tel.: +7-095 323 9272; fax: +7-095 324 3165/324 3165.
E-mail address: chernov@phm.mephi.ru (I.I. Chernov).

0022-3115/$ - see front matter
doi:10.1016/j.jnucmat.2003.08.010

Table 1
The chemical composition of commercial steels

Steel	Chemical content, wt%								
	C	Si	Mn	Cr	Ni	Mo	V	B	Other
Cr12MoWSiNbVCeB (EP-823)	0.14–0.18	1.0–1.3	0.5–0.8	10.0–12.0	0.5–0.8	0.6–0.9	0.2– 0.4	0.006	0.1Ce(0.5–0.8)W(0.2–0.4)Nb
Cr12MoWSiNbVCeNB (EP-900)	0.14–0.18	1.0–1.3	0.6–0.9	10.0–12.0	0.5–0.8	0.6–0.9	0.2– 0.4	0.006	0.1Ce(0.5–0.8)W(0.2–0.4)Nb(0.06–0.01)N
Cr16Ni15Mo2Mn2TiVB (ChS-68)	0.06	0.5	1.6	16.3	14.8	2.2	0.2	0.004	0.35Ti
Cr18Ni10Ti	0.08–0.12	0.3–0.7	1.0–1.2	17.9	9.2–10.1	–	–	–	(0.4–0.5)Ti

The samples ($55\times5\times0.2$ mm^3) were irradiated under identical conditions by 40-keV He^+ ions up to a fluence of 5×10^{20} m^{-2} at 920 K. Microstructural investigations were performed by transmission electron microscope (TEM) JEM-2000EX.

3. Results and discussion

3.1. Model alloys

The typical microstructures and helium bubble parameters formed in irradiated specimens are presented in Fig. 1 and Table 2, respectively. As can be seen in Fig. 1(a) and (b), the bubbles are uniformly distributed in pure nickel and in the matrix of Fe–C alloys containing low concentration of carbon ($N_C \leqslant 0.01$ wt%). The alloys with 0.1–0.4% have martensitic structure after quenching. During the high temperature irradiation a decomposition of the primary structure in these alloys took place, which results in the simultaneous formation of a ferritic–cementitic mixture and bubbles. Because the time of exposure under irradiation at 920 K is short (about 10 min) the decomposition of structure is partial, and the alloys become ferritic–martensitic. Under such conditions an inhomogeneous bubbles distribution has been observed in ferritic and martensitic grains. In ferritic Fe–0.008%C alloy, large faceted bubbles are formed (Fig. 1(b)), and in martensitic alloys small spherical bubbles (Fig. 1(c)). Note that the bubbles parameters in ferrite and ferritic grains of ferritic–martensitic alloys are equal for all specimens within the calculation error (Table 2).

Another feature of bubble structure in ferritic–martensitic alloys is formation of large bubbles on the dislocations in the martensitic grains and an accumulation of bubbles on the interface of ferritic and martensitic grains (Fig. 1(c)), during which ordered distribution of bubbles is observed in the local volumes of martensitic grains (Fig. 1(d)).

3.2. Steels

Typical microstructures of quenched and irradiated commercial steels are presented in Fig. 2. Microstructures of steels irradiated after tempering are shown in Fig. 3. Comparative data of formed helium bubbles parameters are presented in Table 3.

The bubbles of a smaller diameter and with a significantly higher density are observed in austenitic steel ChS-68 after ion implantation of quenched samples in comparison with those in ferritic–martensitic steels. As this takes place, small spherical bubbles are uniformly distributed in the matrix of austenitic steels (Fig. 2(c) and (d)) and the distribution of large faceted bubbles is very non-uniform in ferritic–martensitic steels (Fig. 2(a)

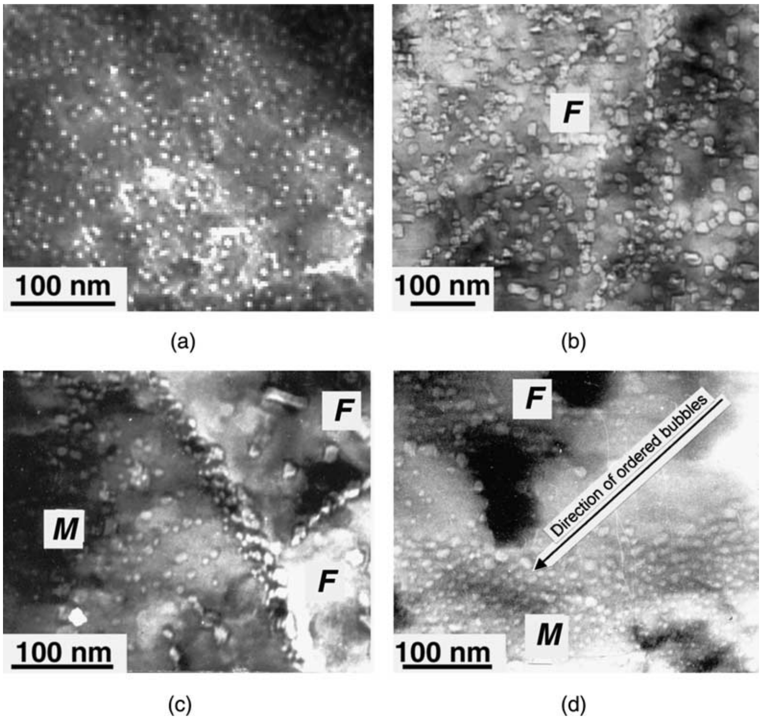

Fig. 1. Helium bubbles in the quenched alloys: (a) Ni, (b) Fe–0.008%C (ferrite), (c) Fe–0.4%C (ferrite and martensite), (d) ordered bubbles in martensite.

Table 2
Helium bubble parameters in Ni and Fe–C alloys (d_{max} and $\bar{d}$ – maximal and average sizes, ρ – volume density, S – swelling of irradiated layer)

No.	Alloy	Heat treatment	d_{max}, nm	$\bar{d}$, nm	ρ, 10^{22} m^{-3}	S, %
1	Ni	Q	~11	6.9	3.7 ± 1.2	0.7 ± 0.2
		Q + A	~18	12.9	1.2 ± 0.4	1.6 ± 0.5
2	Fe–0.008 (F)	Q	~42	15	1.1 ± 0.3	5.1 ± 1.7
3	Fe–0.02 (F)	Q	~20	11	1.6 ± 0.5	1.8 ± 0.6
4	Fe–0.1 (F)	Q	~22	11	1.4 ± 0.5	2.0 ± 0.7
	Fe–0.1 (M)	Q	~12	7.3	3.0 ± 1.0	1.0 ± 0.3
5	Fe–0.4 (F)	Q	~23	11.7	1.8 ± 0.6	2.2 ± 0.7
	Fe–0.4 (M)	Q	~13	3.9	5.5 ± 1.8	0.3 ± 0.1
		Q + A	~18	9.5	2.5 ± 0.8	1.8 ± 0.6

F – ferritic grains; M – martensitic grains; Q – quenching; A – quenching + annealing.

and (b)). The gaseous swelling of steels EP-823 and EP-900 is greater than that for steel ChS-68, the larger bubble diameter in austenitic steel Cr18Ni10Ti giving a higher swelling level then that for steel ChS-68 (Table 3).

Assuming that in the ferritic–martensitic steels, as well as in the model Fe–C alloys, large faceted bubbles are equilibrium with the internal gas pressure, the amount of helium atoms in the bubbles was calculated according to the equation [2]:

$$P = 0.492\exp(5.15 \times 10^{-23} N/V) = 2\gamma/r,$$

where P – pressure, N – the amount of gaseous atoms, V – the total volume of bubbles, γ – surface tension, r – bubble radius. The calculation showed that with this assumption the gaseous atoms amount in the bubbles should be greater than under the ion implantation. Therefore the faceted bubbles are underpressurized in ferritic–martensitic steels, while the small spherical bubbles are overpressurized in austenitic steels.

The standard heat treatment for ferritic–martensitic steels of the 13Cr type (quenching plus tempering at 990–1020 K), as in case of the quenched and tempered

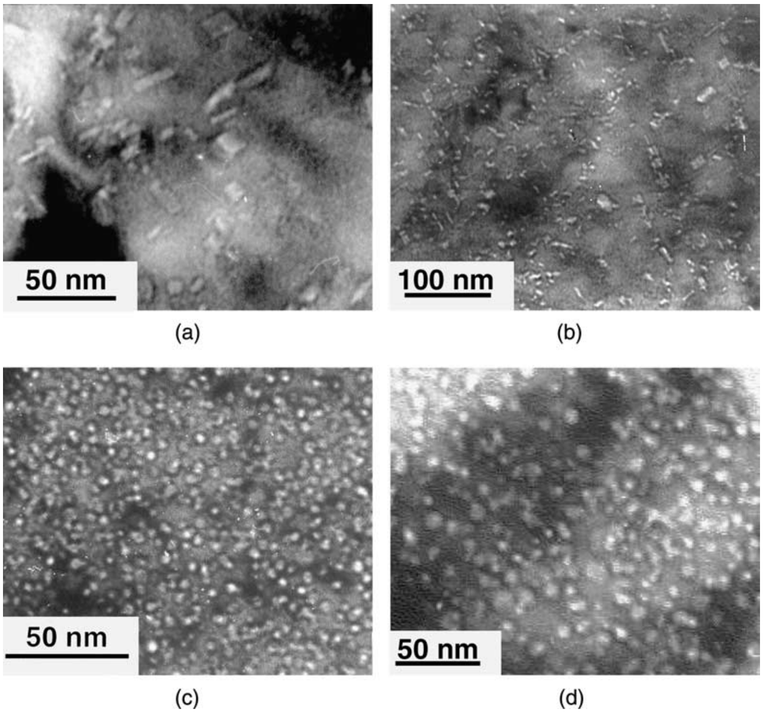

Fig. 2. Helium bubbles in the quenched steels: (a) EP-823, (b) EP-900, (c) ChS-68, (d) Cr18Ni10Ti.

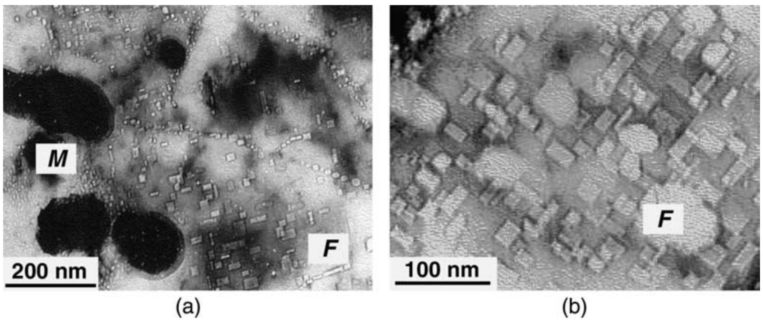

Fig. 3. Helium bubbles in the aged steel EP-900 (a, b).

model Fe–C alloys, leads to a large porosity formation (Fig. 3(a) and (b)). At that, as in case of Fe–C alloys, the larger bubbles and gaseous swelling were observed in ferritic grains of steel (Table 3). Although the primary annealing of quenched austenitic steels also increases the bubble diameters (by the order of magnitude) than under irradiation at quenched condition, nevertheless, the gaseous swelling of tempered ferritic–martensitic steel is significantly larger than that of annealed austenitic steels (Table 3).

After high temperature quenching, a concentration of vacancies in samples corresponds to the thermally steady-state concentration at this temperature, and even at the highest cooling rates ($\sim 10^4$ K/s) a substantial portion of monovacancies combine to form divacancies and, may be, more complicated complexes. After tempering of quenched samples at 990 K the vacancies concentration decrease on some orders of magnitude and these defects are monovacancies for the most part [3]. Therefore under the He^+-ions irradiation of quenched samples the portion of bubbles nucleation centers is substantially higher, which result in higher bubble density and smaller size is in primary quenched steels than those in tempered samples (Table 3).

At equal homologous temperatures the migration activation energy of vacancies E_V^m is less in bcc metals than in metals with fcc structure (for example, the $E_V^m \approx 0.5$–1.5 eV and 1.0–1.6 eV for α-Fe and γ-Fe

Table 3
Helium bubble parameters in the irradiated steels

No.	Alloy	Heat treatment	d_{max}, nm	$\bar{d}$, nm	ρ, 10^{22} m^{-3}	S, %
1	EP-823	Q	~14	4.2	5.9 ± 1.8	0.43 ± 0.13
2	EP-900	Q	~16	3.9	3.1 ± 0.9	0.22 ± 0.07
	EP-900					
	Ferritic grains	Q + A	~40	15.1	1.2 ± 0.4	5.2 ± 1.6
	Martensitic grains		~20	4.2	5.6 ± 1.8	0.85 ± 0.25
3	ChS-68	Q	~5	2.1	27 ± 9	0.14 ± 0.05
		Q + A	~12	8.1	5.3 ± 1.8	1.6 ± 0.5
4	Cr18Ni10Ti	Q	~15	3.6	6.9 ± 2.3	0.49 ± 0.15

correspondingly [4]). It gives rise to more intensive spontaneous point defects recombination in bcc metals and is one of the reasons of lower swelling for ferritic steels. However, this corresponds to the case of steels swelling with a low level of helium generation (irradiation in reactor) or to the absence of helium (heavy ion irradiation). In the presence of helium and simultaneous radiation damage of structure, the intensity of recombination of vacancies and interstitial atoms decreases as helium atoms are captured by vacancies. The higher value of binding energy for helium–vacancy complexes and mobility of vacancies and helium atoms in bcc metals [5–7] promote a rapid growth of bubbles in ferritic steels. Moreover, the rapid growth of bubbles in ferrite may be a result of their coalescence also [8], since smaller self-diffusion activation energy, than in austenite, promotes the higher migration rate of bubbles. As a result of carbon oversaturation the martensitic grains have body centered tetragonal crystal lattice with high internal stresses. It is one of the reason to cause this great difference in parameters of bubbles for ferritic and martensitic grains.

4. Conclusions

1. Under high temperature helium-ion irradiation, maximal gaseous swelling has been observed for ferritic steels and ferritic grains of ferritic–martensitic steels and alloys, and minimal level of swelling for their martensitic grains.
2. The bubbles have a tendency to ordered distribution in martensitic grains.
3. Under high temperature helium-ion irradiation, larger bubbles are formed and higher gaseous swelling is observed in quenched ferritic–martensitic steels EP-823 and EP-900 than in austenitic steel ChS-68. Thus the gaseous swelling of ferritic–martensitic steels may be high and exceed the gaseous swelling for some austenitic steels.
4. The standard heat-treatment (quenching + tempering) of ferritic–martensitic steels, as well as the annealing of austenitic steels, results in an increase of gaseous swelling that significantly exceeds the swelling of quenched steels. In the same condition, the swelling of ferritic grains is several times higher than that of martensitic grains.

References

[1] A.N. Kalashnikov, B.A. Kalin, I.V. Reutov, et al., Phys. Met. Met. Sci. 7 (1990) 203 (in Russian).
[2] S.E. Donnelly, Radiat. Eff. 90 (1985) 1.
[3] A.C. Damask, G.J. Dienes, Point Defects in Metals, Gordon and Breach Science, New York and London, 1963.
[4] N.M. Beskorovainy, B.A. Kalin, P.A. Platonov, I.I. Chernov, Structural Materials for Nuclear Reactors, Energoatomizdat, Moscow, 1995.
[5] W.F.W.M. Van Heugten, F.V.D. Berg, L.M. Caspers, A. Van Veen, Delft. Progr. Rep. Ser.: Phys. Phys. Eng. 3 (1978) 97.
[6] W.D. Wilson, C.L. Bisson, M.I. Baskes, Phys. Rev. B 24 (1981) 5616.
[7] G.J. Thomas, Radiat. Eff. 78 (1983) 37.
[8] B.N. Singh, H. Trinkaus, J. Nucl. Mater. 186 (1992) 153.